Video Article

Glycan Node Analysis: A Bottom-up Approach to Glycomics

Sahba Zaare[1], Jesús S. Aguilar[1], Yueming Hu[1], Shadi Ferdosi[1], Chad R. Borges[1]

[1]Department of Chemistry & Biochemistry, The Biodesign Institute – Center for Personalized Diagnostics, Arizona State University

Correspondence to: Chad R. Borges at Chad.Borges@asu.edu

URL: https://www.jove.com/video/53961
DOI: doi:10.3791/53961

Keywords: Chemistry, Issue 111, glycobiology, glycans, glycosyltransferase, cancer, permethylation, mass spectrometry (MS), gas chromatography (GC), glycoproteins, *O*-linked glycans, *N*-linked glycans

Date Published: 5/22/2016

Citation: Zaare, S., Aguilar, J.S., Hu, Y., Ferdosi, S., Borges, C.R. Glycan Node Analysis: A Bottom-up Approach to Glycomics. *J. Vis. Exp.* (111), e53961, doi:10.3791/53961 (2016).

Abstract

Synthesized in a non-template-driven process by enzymes called glycosyltransferases, glycans are key players in various significant intra- and extracellular events. Many pathological conditions, notably cancer, affect gene expression, which can in turn deregulate the relative abundance and activity levels of glycoside hydrolase and glycosyltransferase enzymes. Unique aberrant whole glycans resulting from deregulated glycosyltransferase(s) are often present in trace quantities within complex biofluids, making their detection difficult and sometimes stochastic. However, with proper sample preparation, one of the oldest forms of mass spectrometry (gas chromatography-mass spectrometry, GC-MS) can routinely detect the collection of branch-point and linkage-specific monosaccharides ("glycan nodes") present in complex biofluids. Complementary to traditional top-down glycomics techniques, the approach discussed herein involves the collection and condensation of each constituent glycan node in a sample into a single independent analytical signal, which provides detailed structural and quantitative information about changes to the glycome as a whole and reveals potentially deregulated glycosyltransferases. Improvements to the permethylation and subsequent liquid/liquid extraction stages provided herein enhance reproducibility and overall yield by facilitating minimal exposure of permethylated glycans to alkaline aqueous conditions. Modifications to the acetylation stage further increase the extent of reaction and overall yield. Despite their reproducibility, the overall yields of *N*-acetylhexosamine (HexNAc) partially permethylated alditol acetates (PMAAs) are shown to be inherently lower than their expected theoretical value relative to hexose PMAAs. Calculating the ratio of the area under the extracted ion chromatogram (XIC) for each individual hexose PMAA (or HexNAc PMAA) to the sum of such XIC areas for all hexoses (or HexNAcs) provides a new normalization method that facilitates relative quantification of individual glycan nodes in a sample. Although presently constrained in terms of its absolute limits of detection, this method expedites the analysis of clinical biofluids and shows considerable promise as a complementary approach to traditional top-down glycomics.

Video Link

The video component of this article can be found at https://www.jove.com/video/53961/

Introduction

Glycolipids, glycoproteins, proteoglycans, and glycosaminoglycans constitute the four main classes of complex, heterogeneous carbohydrates collectively known as glycans. As ubiquitous and integral components of the plasma membrane, glycocalyx, and extracellular matrix and fluids, glycans partake in such diverse biochemical processes as endocytosis, intracellular trafficking, cell motility, signal transduction, molecular recognition, receptor activation, cell adhesion, host-pathogen interaction, intercellular communication, immunosurveillance, and immune response initiation.[1] Present in nearly every domain of life, enzymes known as glycosyltransferases that build glycan polymers act in tandem with glycoside hydrolases (also known as glycosidases, which break down glycans) to construct, remodel, and ultimately produce finalized glycan polymers [2]. Although each glycosyltransferase may operate on different glycoconjugates, a glycosyltransferase generally forges a linkage- and anomer-specific glycosidic bond by transferring the monosaccharide moiety of a particular activated nucleotide sugar donor (*e.g.,* GDP-fucose) to a certain category of nucleophilic acceptors (*e.g.,* a lipid, polypeptide, nucleic acid, or growing oligosaccharide). It has been estimated that more than 50% of proteins (especially membrane and secretory proteins) are post-translationally modified by glycosylation.[3] Rudimentary combinatorial calculations provide an appreciation for the considerable variability, versatility, and specificity accorded to glycoproteins by glycosylation; for example, if a polypeptide substrate has only 10 glycosylation sites and each site can form a glycosidic linkage with 1 of only 3 different monosaccharide reducing ends, then, theoretically, the final glycoprotein can assume 3^{10} = 59,049 distinct identities. In glycoproteins, glycosidic linkages commonly form with the side-chain nitrogen of asparagine residues in the sequence Asn-X-Ser/Thr (X can be any amino acid except proline) to yield *N*-glycans[2] and side-chain hydroxyls of serine and threonine residues to yield *O*-glycans[4]. The composition of a cell's glycome (*i.e.,* its complement of glycosylation products) is unique and limited because, with few exceptions, glycosyltransferases exhibit strict donor, acceptor, and linkage specificity.[5] Important and abundant blood plasma glycoproteins suffer aberrant glycosylation as a downstream consequence of abnormal glycosyltransferase expression and activity due to many pathological conditions, especially cancer and inflammatory diseases.[6-24]

Mainly due to epigenetic factors, the glycome is significantly more diverse, dynamic, and complex than the proteome and transcriptome.[25,26] While approximately 1% of the mammalian genome encodes the formation, modification, and assembly of glycans,[27] glycosylation proceeds in a non-template-driven manner-a marked contrast to polypeptide and nucleic acid biosynthesis. The interplay among the relative quantity

Copyright © 2016 Journal of Visualized Experiments

and activity of glycosylation enzymes and such environmental factors as nutrient and precursor availability ultimately determines the nature, rate, and extent of glycosylation.[5,28] Embryogenesis (*e.g.,* determination and differentiation), cellular activation, and progression through the cell cycle influence gene expression (*i.e.,* transcription and translation) and alter the identity and quantity of available glycosyltransferases, whose activity is the immediate upstream determinant of the cell's glycan profile. Because (some of) the proliferative, adhesive, and invasive properties of cancerous cells resemble those of ordinary embryogenic cells, specific changes in glycan biosynthetic pathways (*e.g.,* precursor accumulation, deregulated expression, aberrant modification, structural truncation, or novel formation) serve as universal cancer biomarkers that indicate various stages of tumor formation, progression, migration, and invasion.[29] Although glycosylation is highly complex, evidently only a few alterations in glycosylation can enable carcinogenesis and metastasis; apparently, certain "aberrant" glycosylation products indeed benefit cancerous cells by enabling them to evade immune recognition and survive the demands of migration in inhospitable intravascular and metastatic environments.[28,30,31] Not surprisingly, experiments have revealed that disrupting or preventing patterns of altered gene expression and aberrant glycan formation can halt tumorigenesis.[29] Nonetheless, the aberrant glycans detected in a biofluid sample (*e.g.,* urine, saliva, and blood plasma or serum) may not be direct indicators of cancer (or another disease), but rather downstream outcomes of subtle yet significant changes in the immune system or quantifiable ramifications of a pernicious condition in an unpredictable organ.[32]

Although they provide universal information about the glycome, many molecular interaction-based glycomics techniques (*e.g.,* lectin/antibody arrays and metabolic/covalent labeling) depend upon the detection of whole glycan structures and do not provide detailed structural information about individual glycans. In marked contrast, mass spectrometry (MS) can help identify and quantify individual glycan structures and reveal such structural information as the attachment sites to polypeptide cores. Deregulated expression or activity of only one glycosyltransferase can initiate a cascade of detrimental molecular events in multiple glycosylation pathways. Because each glycosyltransferase may operate on more than one glycoconjugate substrate and across different growing glycan polymers, deregulated biosynthetic cascades yield disproportionally increased amounts of only one glycan product but several heterogeneous classes of aberrant glycans in intra- or extracellular fluids.[33] However, such unique aberrant glycans are sometimes considered impractical as biomarkers for cancer or other glycan-affective pathologies because, compared to the large pool of well-regulated glycans, these aberrant glycans represent a very small fraction that may often remain undetectable even by such highly sensitive techniques as mass spectrometry. For example, in intra- and extracellular body fluids, the broad protein-concentration spectrum (which spans eight orders of magnitude) can prevent detection of scarce glycoproteins that are masked by the more abundant species. [32] Moreover, determining glycosyltransferase activity remains a considerable practical and theoretical challenge because many glycosyltransferases are absent in clinical biofluids or become inactive *ex vivo*. Despite the difficulty of consistently detecting and quantifying ultra-minute quantities of unique whole glycans, practitioners of mass spectrometry have made enormous strides toward employing intact glycans as clinical markers. We have recently developed a complementary approach to the analysis of intact glycans that, employing GC-MS, facilitates the detection of all constituent branch-point and linkage-specific monosaccharides ("glycan nodes") that together impart uniqueness to each glycan and in many cases directly serve as molecular surrogates that quantify the relative activity of the culpable glycosyltransferase(s).

Since its first reported direct application to glycan analysis in 1958, gas chromatography (GC) has proven a powerful technique to analyze per-methylated mono- and disaccharides,[34] determine their anomericity and absolute configuration, and separate them for subsequent mass spectrometric analysis.[35] Between 1984 and 2007, Ciucanu and colleagues introduced and refined a solid-phase glycan permethylation technique that employed sodium hydroxide and iodomethane, followed by liquid/liquid extraction of permethylated glycans using water and chloroform.[35,36] Between 2005 and 2008, Kang and co-workers integrated a time-saving spin-column approach into the permethylation step.[37,38] In 2008, the Goetz research group devised a quantitative solid-phase permethylation glycan-profiling method using matrix-assisted laser desorption-ionization (MALDI) mass spectrometry to compare and potentially distinguish invasive and non-invasive breast cancer cells;[39] then, in 2009, the Goetz team combined enzymatic and chemical release techniques to cleave *O*-glycans from intact glycoproteins in a highly alkaline solid-phase permethylation scheme.[40] Although the Goetz procedure facilitated simultaneous permethylation and chemical release of *O*-glycans, it was applied only to pre-isolated glycoproteins. We modified this technique in 2013 and adapted it for whole unfractionated biofluids and homogenized tissue samples by incorporating trifluoroacetic acid (TFA) hydrolysis, reduction, and acetylation steps.[33] These additional steps also release glycans from glycolipids and *N*-linked glycans from glycoproteins and convert them into partially methylated alditol acetates (PMAAs, **Figure 1**), whose distinctive methylation-and-acetylation patterns facilitate analysis by GC-MS and uniquely characterize the constituent glycan nodes in the original intact glycan polymer[41] (**Figure 2**).[33] Ultimately, this procedure produces a composite portrait of all the glycans in a complex biofluid based on direct, relative quantification of unique glycan features such as "core fucosylation", "6-sialylation", "bisecting GlcNAc", and "beta 1-6 branching"-each derived from a single GC-MS chromatographic peak. This article presents further optimization of the permethylation, acetylation, isolation, and clean-up stages along with improvements in the mode of relative quantification.

Protocol

Caution: Avoid skin/eye contact with any of the reagents used in this experiment. Upon exposure, thoroughly flush the affected area with water and seek immediate medical advice.

1. Permethylation and Glycan Extraction

1. **Column Preparation**
    1. Obtain as many microfuge spin column units as the samples to be analyzed. Break and detach the plastic reservoir tube caps. Place a microfuge mini filter in each reservoir tube. Place the assembled microfuge spin columns (containing the mini filters) in a microfuge tube rack.
    2. Obtain a stock of sodium hydroxide (NaOH) beads (20-40 mesh). Transfer some NaOH to a small weighing boat or, if humidity is causing clumping, a hot porcelain mortar as the working stock of NaOH. Avoid using clumps of NaOH or crushed/powdered NaOH beads.
    Caution: NaOH is a potent toxin and corrosive base. Flush exposed skin/eyes with water for 15 min. Thoroughly clean the workbench after completing the experiment.
    3. Using a small scoop or spatula, transfer NaOH beads from the working stock to fill the microfuge mini filters with NaOH up to the first outer bevel (~5 mm below the brim). Tap the filled microfuge filters on the bench-top to pack/condense the NaOH beads.

Note: Throughout this experiment, to minimize excessive water adsorption by hygroscopic NaOH beads, maintain the level of any added fluids (*e.g.,* acetonitrile, dimethyl sulfoxide, analyte solution) above the surface of the NaOH column packing and limit direct contact with air.

4. Obtain a stock of acetonitrile (ACN). Transfer ~350 µl ACN to each NaOH-packed microfuge mini filter. Keep the NaOH submerged under ACN and remove large air bubbles by stirring with a tip-crimped gel-loading pipette tip.
   Caution: Acetonitrile is a flammable irritant.
5. **Column Centrifugation**
   1. Arrange the microfuge columns symmetrically inside a centrifuge; use a balance tube if necessary. Avoid spilling any NaOH granules inside the centrifuge. Close the centrifuge lid.
   2. Centrifuge the columns (containing NaOH and ACN) for ~15 sec at 2,400 × g.
   3. Upon completion of centrifugation, remove microfuge columns from the centrifuge, and discard the ACN into a hazardous waste container. Keep the NaOH column packing intact.
6. Add ~350 µl dimethyl sulfoxide (DMSO) to each NaOH-packed microfuge mini filter. Keep the NaOH submerged under DMSO and remove any large air bubbles with a pipette tip. As previously described, centrifuge columns for ~15 sec at 2,400 × g, and discard the DMSO while keeping the NaOH packing intact.
   Caution: DMSO is a mutagen and irritant and is easily absorbed through the skin.
7. Plug all microfuge mini filters with the plugs included in the spin filter kit. Transfer ~350 µl DMSO to each NaOH-packed microfuge mini filter and use a 200 µl pipette tip to remove air bubbles in the NaOH packing so that DMSO reaches all regions within then NaOH packing. Avoid crushing or excessively scraping the NaOH beads; NaOH powder is undesirable. Finish this step as rapidly as possible.

2. **Preparation of Plasma Quality Control (QC) Sample(s)**
   Note: To ensure consistent results across experimental batches, consider using at least one aliquot of a sample taken from a large, homogeneous bulk collection of the biological material of interest to be analyzed in each batch. For example, if analyzing blood plasma, use aliquot(s) of a bulk collection of blood plasma as the QC sample(s) in each batch. Process QC samples in the same manner as unknown samples.
   1. Centrifuge a stock sample of QC plasma for 4 min at ~10,000 × g. During centrifugation, some high-density precipitate may settle to the bottom and some low density precipitate may float to the top of the plasma. Avoid both when removing aliquot(s) of plasma.
   2. Proceed to "1.3) Sample Preparation" below. Then, return to this step after plasma centrifugation is complete.
   3. Withdraw 9 µl of centrifuged QC plasma and transfer it to an appropriately labeled 1.5-ml polypropylene test tube equipped with a snap-shut cap (hereafter referred to as "1.5-ml plastic test tube"). Add 1 µl of deionized water to each aliquot; if desired, use this as a carrier for internal standard(s).
   4. Add 270 µl DMSO to this plasma control. Vortex to ensure complete dissolution.

3. **Sample Preparation**
   1. Obtain as many 1.5-ml plastic test tubes as the number of biological (analyte) samples.
   2. Transfer 9 µl of each biological (analyte) sample to its corresponding 1.5-ml plastic test tube. Transfer 1 µl of deionized water and 270 µl DMSO to each sample tube.
   3. Vigorously mix (*e.g.,* vortex and/or repeatedly pipette up and down) the samples to ensure complete dissolution in DMSO.
      Caution: Perform the following steps inside a fume hood. Used in the following steps, iodomethane (CH_3I), dichloromethane (CH_2Cl_2, a.k.a. methylene chloride), and chloroform ($CHCl_3$, trichloromethane), are volatile liquids capable of dissolving certain types of plastic (*e.g.,* nitrile gloves). Be sure to use solvent-resistant gloves. Due to their low viscosity and high vapor pressure, these reagents can drip from a pipette tip during transfer. Minimize reagent loss and potential exposure by holding the stock solution adjacent to the receiving vessel.
   4. Transfer a sufficient total volume of iodomethane to a small, clean tube. Each analyte sample will require 105 µl iodomethane. Transfer ~500 µl dichloromethane into another clean tube. To prevent syringe clogging, rinse the syringe with dichloromethane immediately after iodomethane transfer.
      Caution: Iodomethane is photosensitive, volatile, and potent toxin capable of damaging the central nervous system or causing death if inhaled or ingested. Dichloromethane is a potential carcinogen, reproductive mutagen, and potent irritant capable of damaging several organs or causing death.
   5. Use an analytical syringe to add 105 µl iodomethane to each analyte sample. Cap analyte tubes immediately to minimize iodomethane evaporation. Thoroughly vortex and, if necessary, briefly centrifuge all samples to ensure that no liquid remains in the cap. Any color change (*e.g.,* to brown, purple, or yellow) signals iodomethane degradation, which may jeopardize the following permethylation reaction.
   6. Rinse the analytical syringe used to transfer iodomethane with dichloromethane at least 3 times. This will prevent it from clogging. Dispose of this rinse, along with extra iodomethane and dichloromethane into an organic hazardous waste vessel. Place used test tubes into a hazardous waste container.
   7. Obtain a new set of 2-ml plastic reservoir tubes. Remove snap-caps if desired.
   8. Unplug the microfuge mini filters. Centrifuge the unplugged columns for 15 sec at 2,400 × g, and then discard the reservoir tubes along with the DMSO effluent.
   9. Re-plug the centrifuged spin columns, and place them inside the new reservoir tubes. Number each spin column and its corresponding reservoir tube with the same sample number. Ensure that the mini filter plugs are tight; potential leakage can impact the next step. Minimize the time between removing DMSO from the spin columns and transferring the analyte samples onto the spin columns.
   10. **Permethylation**
      1. Quantitatively transfer each sample solution to its corresponding NaOH-bead-filled microfuge spin column. Use a 1,000-µl pipette tip for this step. Following transfer, crimp ~2 mm of the end of a 200 µl tip and leave it in the column contents to use as a stirrer. Repeat for all samples.
         Note: The low viscosity of iodomethane can cause sample loss because the analyte solution can drip from the pipette tip during the transfer. Hold the sample tube and the spin column adjacent to each other with one hand, and rapidly transfer the sample solution with the other hand.

2. Allow the permethylation reaction to proceed for 11 min. Stir each sample at least 4-5 times during this period. To facilitate efficient permethylation, which occurs at the surface of NaOH beads, use tip-crimped gel-loading pipette tips as stirrers to gently mix the column contents. Aggressive mixing can puncture the spin filter, pulverize and suspend NaOH beads (which can reduce the effectiveness of subsequent liquid/liquid extraction), and/or cause sample loss (as the sample-soaked NaOH granules can overflow from the column).
3. In preparation for the subsequent liquid/liquid extraction step, prepare a sufficient amount of 0.5 M sodium chloride (NaCl) solution in a 0.2 M sodium phosphate buffer (pH 7.0), to be stored at room temperature. Each sample will require a total of ~12 ml NaCl solution for all three cycles of liquid/liquid extraction.
4. Upon completion of the 11-min permethylation period, immediately yet carefully unplug the columns and centrifuge them for 15 sec at 2,400 × g. Discard the plugs.

11. Immediately remove spin columns from the centrifuge and place them into a new set of empty spin reservoir tubes, leaving the flow-through solution containing freshly permethylated glycans behind. Do not discard anything.
12. As soon as possible, add 300 µl acetonitrile (ACN) to the dry, NaOH-filled spin filters. Centrifuge the spin filters for 30 sec at 9,600 × g.
13. Immediately thereafter, transfer the main permethylation solution (*i.e.*, the solution that was incubated with the NaOH beads for 11 min then spun through the spin filter into a centrifuge tube prior to addition of 300 µl of ACN in the previous step) to silanized 13 x 100 mm glass test tubes[42] containing 3.5 ml of 0.2 M sodium phosphate buffer containing 0.5 M NaCl, pH 7.0 and mix (vortex) immediately. Avoid transferring any solid white residue during this step. Do this for each sample before proceeding to the next step.
14. Without delay, transfer (combine) the ACN spin-through in each reservoir tube to (with) the rest of the liquid sample in its respective silanized glass tube and mix (vortex) immediately. Again, avoid transferring any solid white residue during this step. Cap, shake, and vortex the glass tube. Repeat for each sample. Discard the NaOH columns and Pasteur pipettes in appropriate waste containers.

4. **Liquid/Liquid Extraction and Glycan Purification**
   1. Inside the fume hood, add 1.2 ml chloroform to each sample. Immediately thereafter, cap the silanized glass tubes and vigorously mix the contents.
   2. Pre-heat metal blocks to approximately 75 °C in an evaporation manifold. Use heating blocks with wells that can accommodate the 13 mm × 100 mm glass tubes.
   3. Obtain a new set of silanized Pasteur pipettes, non-silanized Pasteur pipettes, and silanized glass test tubes with caps.
      Caution: Chloroform ($CHCl_3$) is an irritant, mutagen, and potential carcinogen capable of permeating through some types of gloves.
   4. Briefly centrifuge (~3,000 × g) sample-containing glass tubes to separate the aqueous and organic layers.
   5. Use a non-silanized Pasteur pipette to extract enough of the top aqueous layer such that ~3 mm of the aqueous layer remains above the bottom organic layer.
   6. Add 3.5 ml of the 0.5 M NaCl solution in a 0.2 M sodium phosphate buffer (pH 7) to each glass tube, vigorously mix, and briefly centrifuge (~3,000 × g). As in the previous step (1.4.3), use a non-silanized Pasteur pipette to extract the aqueous layer.
   7. Repeat the previous step (1.4.4), but leave ~1 ml of the aqueous layer.
   8. Use a clean silanized Pasteur pipette to transfer the organic layer to a clean and appropriately labeled silanized 13×100 mm glass test tube. Avoid aqueous contamination by extracting in the following way:
      1. Hold both the current and new silanized glass test tubes adjacent to each other in one hand. With the other hand, press the pipette bulb to create bubbles while inserting the pipette down through the aqueous layer.
      2. Once inside the organic layer, stop creating bubbles, and hold the pipette bulb steady to allow the organic and aqueous layers to stabilize and separate again. Then, slowly release the bulb to withdraw as much of the organic layer as possible without any aqueous contamination.
      3. Rapidly raise the pipette tip through the aqueous layer, and resist the natural reflex of slightly releasing the bulb (which results in withdrawing some aqueous contamination) while raising the pipette out of the tube.
      4. Rapidly transfer the low-viscosity organic layer to the adjacent new tube. Any aqueous contamination will be visible as small liquid droplets on top of the extracted organic layer in the new glass tubes. If aqueous/NaCl contamination is visible, remove it with a pipette; centrifuge if needed to pool the aqueous droplets into a single droplet.

   9. Properly dispose of old glass tubes, pipettes, and aqueous and organic waste solutions. Wash and recycle glass tube caps.
   10. Dry all samples under a gentle and constant stream of nitrogen in a preheated evaporation manifold at 75 °C for ~5 min inside a fume hood. To ensure evaporative cooling during all dry-down steps, a gentle and constant flow of nitrogen must disturb the liquid surface without splashing or spattering the liquid. Remove samples from the evaporation manifold upon complete drying of the final sample. White specks at the bottom of a dried glass tubes indicate buffer/NaCl contamination.
   11. Pause the procedure here if there is not enough time remaining in the day to complete the TFA hydrolysis step. Temporarily (*i.e.*, overnight) store dry samples at -20 °C. To continue the procedure after storage, remove the samples from the -20 °C freezer and allow them to warm completely before uncapping.
   12. While samples warm, in preparation for trifluoroacetic acid (TFA) hydrolysis (next stage), set the heating mantle such that the temperature of the liquid test-tube contents will reach 121 °C. Prepare the TFA solution from TFA stock (see Step 2.1 below).

2. Trifluoroacetic Acid (TFA) Hydrolysis

Caution: Trifluoroacetic acid (TFA) is a corrosive organic acid and toxic irritant.

1. Prepare a sufficient amount of a 2.0 M TFA solution in deionized water. Each analyte sample will require 325 µl of 2.0 M TFA solution. Concentrated TFA is 13.0 M.
2. Add 325 µl of 2.0 M TFA to each analyte sample. To prevent TFA evaporation and sample loss during the subsequent drying step (2.3 below), tightly cap each sample tube immediately after adding TFA. Mark the solution level in all glass tubes. Vortex each sample thoroughly before the next step.

3. Incubate the tightly capped sample tubes for 2 hr in a suitable pre-heated heating block or oven such that the contents reach a temperature of 121 °C. If using a heating block instead of an oven, cover sample tubes with aluminum foil to prevent condensation of TFA at the top of the tube and partial drying of sample residue at the bottom of the tube. Check the sample solution levels after 20-30 min. to ensure minimal TFA evaporation. If necessary, tighten the caps further or replace caps for a tighter fit.
4. During the 2-hr wait, set another evaporation manifold to 75 °C for the next step (see 2.4 below).
5. When the 2-hr heating period is complete, dry samples at 75 °C under a gentle stream of nitrogen gas for ~15 min. Do not leave samples unattended for more than 15 min. Frequently check samples, and discontinue heating and drying once all samples are dry.
6. Pause the procedure here if there is not enough time remaining in the day to complete the reduction step. Temporarily (*i.e.*, overnight) store samples at -80 °C. To continue the procedure after storage, remove the samples from the -80°C freezer, and allow them to warm completely before uncapping.

3. Reduction

1. Inside a fume hood, prepare a sufficient amount of a 10 g/L sodium borohydride ($NaBH_4$) solution in 1 M ammonium hydroxide (NH_4OH). Each sample will require 475 µl of this solution. Make a **fresh** solution for each batch of samples. Concentrated ammonium hydroxide (27-30% w/w NH_3) is approximately 14.5 M.
   Caution: Sodium borohydride ($NaBH_4$) is a hygroscopic, water-reactive toxin and potent irritant that releases-upon contact with water-highly flammable vapors that cause serious burns upon inhalation, ingestion, or eye/skin contact.
   Caution: Ammonium hydroxide (NH_4OH) is a corrosive irritant and toxin capable of causing severe burns and irreversible organ damage upon inhalation, ingestion, or eye/skin contact. Flush affected areas with water for 30 min, and prevent the victim from rubbing or scratching the affected areas.
2. To each sample, add 475 µl of the 10 g/L $NaBH_4$ in 1 M NH_4OH. Mix samples thoroughly to dissolve any residues. Cap test tubes and allow the reduction reaction to continue for 1 hr.
3. During the 1-hr wait, set the heated evaporation manifold to 75 °C. Use a heating block with appropriate wells for the glass tubes (see 3.4 below).
4. When the 1-hr reaction period is complete, add 63 µl methanol (MeOH) to each sample. This step and the following step remove residual boron as trimethyl borate — a relatively volatile liquid that boils at 68 °C.
5. Dry samples (in the pre-heated manifold) at 75 °C under a gentle stream of nitrogen gas for ~15 min. Frequently check samples and do not leave them unattended. Small liquid droplets at the bottom of the glass tubes indicate that the sample is not yet dry.
   Note: To distinguish air bubbles from liquid droplets, tilt the test tube. Only liquid droplets will move after tilting, but the converse is not always true: if a bubble does not move, it can still be a (very small) liquid droplet.
6. Once samples are completely dry, prepare a 9:1 (v/v) solution of methanol (MeOH) and acetic acid (AcOH). Add 125 µl of this MeOH:AcOH solution to each sample.
7. Dry samples (in a pre-heated manifold) at 75 °C under a gentle stream of nitrogen gas.
8. When samples are completely dry, vacuum-dry the samples for 20 min at room temperature: Place samples into a plastic vacuum tub (such as those sold by FoodSaver), close the vacuum lid, set the vacuum dial to "vacuum," connect the vacuum hose, and turn on the vacuum. To disassemble the vacuum, reverse these steps. Wait for the system to completely decompress before attempting to open the vacuum lid.
9. Pause the procedure here if there is not enough time remaining in the day to complete the reduction step. Temporarily (*i.e.*, overnight) store samples at -80 °C. To continue the procedure after storage, remove the samples from the -80 °C freezer, and allow them to warm completely before uncapping.
10. While waiting for samples to vacuum-dry (or warm, after storage), prepare the reagents for the next step. Obtain and number a silanized conical-bottom autosampler (AS) vial (with cap) for each sample. Moreover, pre-heat both a shallow-well AS-vial heating block and a deep-well glass-tube block such that the glass tube contents will reach a temperature of 50 °C.

4. Acetylation (Performed in a Fume Hood)

1. Add 18 µl deionized water to each sample. Cap and thoroughly vortex all tubes to completely dissolve any precipitates.
2. Add 250 µl acetic anhydride to each glass tube. Cap, thoroughly vortex, and sonicate in a water bath for 2 min to ensure complete dissolution of any residues and precipitates.
3. Cover glass tubes with aluminum foil, and incubate at an internal temperature of 50 °C for 10 min.
4. Add 230 µl concentrated trifluoroacetic acid (TFA) to each sample. Immediately cap and mix the samples. Then, incubate samples-covered with aluminum foil-for 10 min at an internal temperature of 50 °C.
5. After incubation, add 1.8 ml dichloromethane (CH_2Cl_2) to each sample. Cap and mix well.
6. Add 2.0 ml deionized water to each sample. Cap and mix samples well. Centrifuge from 0 to 3,000 × g to separate the layers. Use a non-silanized Pasteur pipette to perform liquid/liquid extraction as outlined in Step 1.4.6, avoiding water contamination.
7. Repeat extraction once more, for a total of two extractions. Use **silanized** Pasteur pipettes to transfer the organic layer into labeled **silanized** AS vials (held securely in an AS rack). Fill the AS vials to just below the brim.
8. Use a pre-heated, shallow-well heating block to dry samples (in AS vials) for 15 min at 40 °C under nitrogen gas. Do not over-dry. Final products are known as partially methylated alditol acetates (PMAAs).

5. Gas Chromatography – Mass Spectrometry (GC-MS)

1. Reconstitute each sample in 100 µl of acetone and mix well. Use an autosampler to inject 1 µl of each sample in split mode into the GC split-mode liner (maintained at 280 °C and containing a small plug of silanized glass wool). Use a split ratio of 40. Use helium as the carrier gas in constant flow mode at 0.8 ml/min through a 30-m DB-5ms GC column with a 0.25 mm ID and 0.25 micron film thickness.
2. Hold the initial GC oven temperature at 165 °C for 0.5 min. Following the initial hold time, program the oven to ramp the temperature, for each run, from 165 °C to 265 °C at a rate of 10 °C/min (which takes 10 min) and then immediately ramp the temperature 265 °C to 325 °C at a rate of 30 °C/min (which takes 2 min) and maintain the temperature at 325 °C for 3 min. The total run time per sample is 15.5 min.

Copyright © 2016 Journal of Visualized Experiments

3. Use a properly tuned and calibrated mass spectrometer to subject the sample components eluting from the GC column to electron ionization (EI, 70 eV at 250 °C). For a TOF mass analyzer, analyze fragments from *m/z* 40 to *m/z* 800 with a 0.1-sec pulse summation rate. Set an EI-filament solvent delay time of 2.5 min.

6. Data Analysis

1. If using a TOF mass analyzer, sum the most abundant and/or diagnostic fragment ions for each PMAA by applying a mass window of 0.15 Da to obtain an extracted ion chromatogram. Target ions for each PMAA have been published elsewhere,[33] but the following alterations have been made: t-Glc ions are now 145.1 + 205.1; 2-Man ions are 161.1 + 189.1; 3-Gal ions are 161.1 + 233.1, 6-Gal ions are 161.1 + 189.1 + 233.1; 2,6-Man ion is 189.1; 3,6-Man ions are 189.1 + 233.1.
2. Use QuanLynx or other software to automatically integrate peak areas for each summed extracted ion chromatogram.
3. Manually verify the integration results by viewing each integrated extracted ion chromatogram. Then, export the peak integration data to a spreadsheet for further analysis and data normalization, which involves dividing the area of each individual hexose XIC by the sum of all hexose XIC areas; likewise, the area of each individual HexNAc XIC is divided by the sum of all HexNAc XIC areas. This procedure produces normalized abundances for each individual hexose and HexNAc.

Representative Results

A total ion current chromatogram (TIC) showing successful permethylation, hydrolysis, reduction, and acetylation of human blood plasma samples relative to cases in which two critical permethylation steps were executed incorrectly are shown in **Figure 3**.

Absolute Yield of HexNAcs Relative to Hexoses:

N-acetylhexosamine (HexNAc) partially methylated alditol acetates (PMAAs) tend to have lower yield than hexoses.[43] To estimate the absolute yield of HexNAcs relative to hexoses, six 10-µg samples of *N*-acetyllactosamine (a Gal1-4GlcNAc disaccharide) in 10 µl of water were analyzed. TIC peak areas for terminal galactose (t-Gal) and 4-GlcNAc were integrated. The percentage of 4-GlcNAc relative to the total amount of t-Gal and 4-GlcNAc was 11.3 ± 0.7% (SEM). Although HexNAc yields are reproducible (see below), the fact that this value is much less than the theoretical value of 0.5 indicates that the yield of HexNAcs is fundamentally lower than that of hexoses. (The HexNAc theoretical yield is 0.5 because *N*-acetyllactosamine is a 1:1 hexose-HexNAc disaccharide.)

Intra- and Interassay Reproducibility:

Intra- and interassay reproducibility for all glycan nodes contributing at least 1% of the total hexose or HexNAc signal are provided in **Table 1**. These data were acquired by 3 separate analysts on 3 separate days, using the same stock of EDTA plasma. Autosampler stability data under this optimized protocol for the 18 most abundant glycan nodes in human plasma (*i.e.*, those with > 1% of the total hexose or HexNAc signal) are provided in **Figure 4**.

Other Notable Observations:

While optimizing the permethylation methodology, we found that it is not necessary to prevent adsorption of water by the NaOH beads prior to initial washing with acetonitrile. We also found that the presence of a small quantity of water during the final acetylation step in combination with a brief period of heating with acetic anhydride without TFA helps to facilitate complete reaction. Finally, the high resolving power of time-of-flight (TOF) mass spectrometry is not necessary for successful glycan node analysis: Initial results based on parallel injection of the same set of samples on a GC-TOF-MS and a traditional transmission quadrupole-based GC-MS operated in selected ion monitoring (SIM) mode demonstrate similar results in terms of the final normalized hexose and HexNAc relative abundances.

Copyright © 2016 Journal of Visualized Experiments

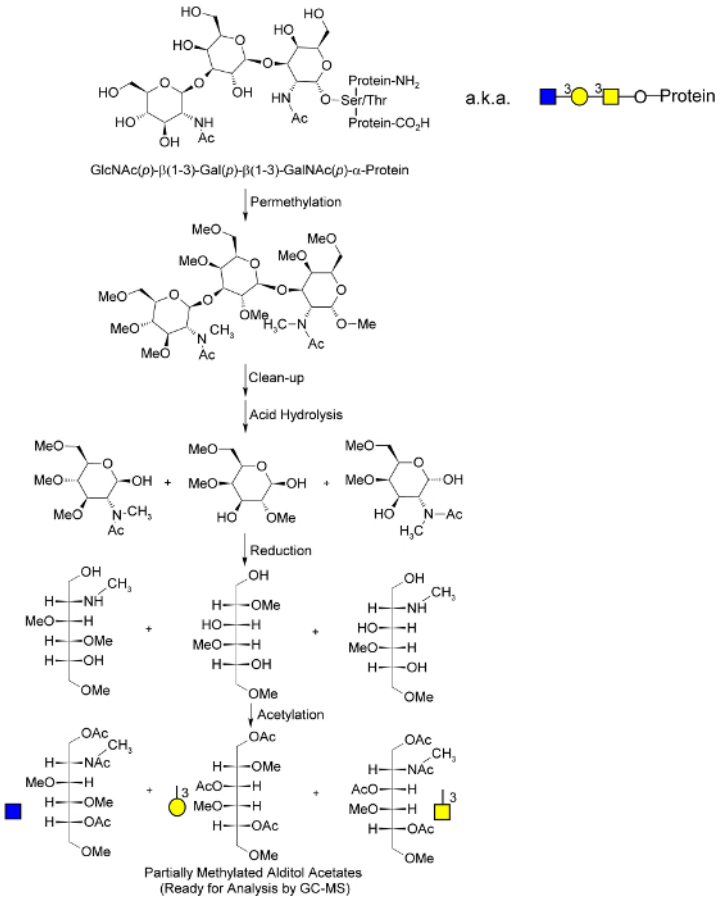

Figure 1. Molecular overview of the global glycan methylation analysis procedure. An *O*-linked glycan is illustrated; these are released during the permethylation process, which has been adapted from Goetz.[40] Following permethylation and hydrolysis, monosaccharides are reduced and nascent hydroxyl groups "marked" by acetylation. The unique pattern of methylation and acetylation in the final partially methylated alditol acetates (PMAAs) corresponds to the unique "glycan node" in the original intact polymer and provides the molecular basis for separation and quantification by GC-MS. *N*-linked and glycolipid glycans are released as linkage-marked monosaccharides during acid hydrolysis. Adapted from Borges *et al.*[33] with permission. Please click here to view a larger version of this figure.

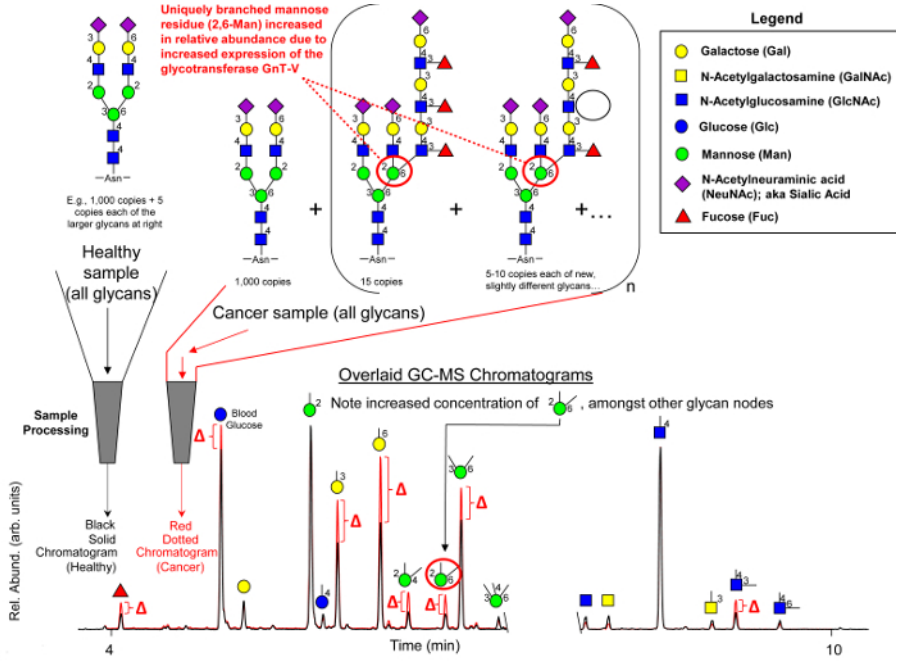

Figure 2. Conceptual overview of the analytical concept. An upregulated glycosyltransferase (*e.g.*, GnT-V) causes an increase in the quantity of a specific, uniquely linked glycan monosaccharide residue (a 2,6-linked Mannose "node" in this example)-which, through the subsequent action of other glycosyltransferases, can lead to formation of a mixture of heterogeneous whole-glycan structures at low copy number each-all of which can be difficult to detect and quantify in routine fashion. Analytically pooling together the "glycan nodes" from amongst all the aberrant glycan structures provides a more direct surrogate measurement of GnT-V activity than any single intact glycan. Simultaneous measurement of *N*-, *O*-, and lipid linked "glycan nodes" in whole biospecimens as described here (and originally elsewhere[33]) represents a conceptually novel means by which to detect and monitor glycan-affective diseases such as cancer. Actual extracted ion chromatograms from 10-microliter blood plasma samples shown. Numbers adjacent to monosaccharide residues in glycan structures indicate the position at which the higher residue is linked to the lower residue. If no linkage positions are indicated in the chromatogram annotation the residue is either in the terminal position or free in solution (*e.g.,* glucose). All residues except sialic acid link downward via their 1-position; sialic acid links downward via its 2-position. Split in chromatogram indicates change in extracted ion chromatograms: m/z 117 +129 for hexose residues and m/z 116 + 158 for *N*-acetylhexosamine (HexNAc) residues. Adapted from Borges *et al.*[33] with permission. Please click here to view a larger version of this figure.

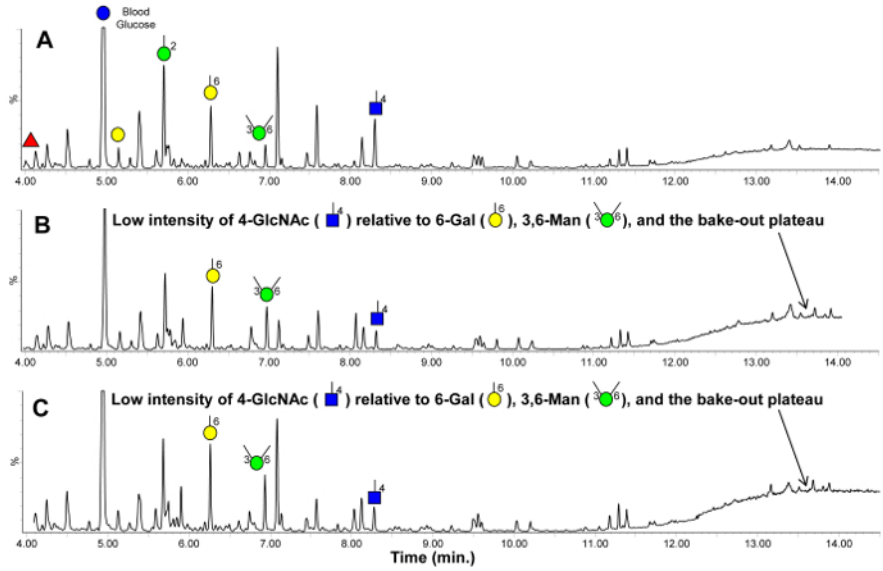

Figure 3. Representative Results. Total ion current chromatograms (TICs) for glycan node analysis of the same human blood EDTA plasma sample in which **A**) the sample was processed correctly, **B**) the white residue in the permethylation solution that was spun through the NaOH column was carried into the subsequent mixture for liquid/liquid extraction, and **C**) the permethylation solution that was spun through the NaOH column was added to the phosphate buffer but not mixed thoroughly prior to addition of chloroform for liquid/liquid extraction. Legend provided in **Figure 2**. Please click here to view a larger version of this figure.

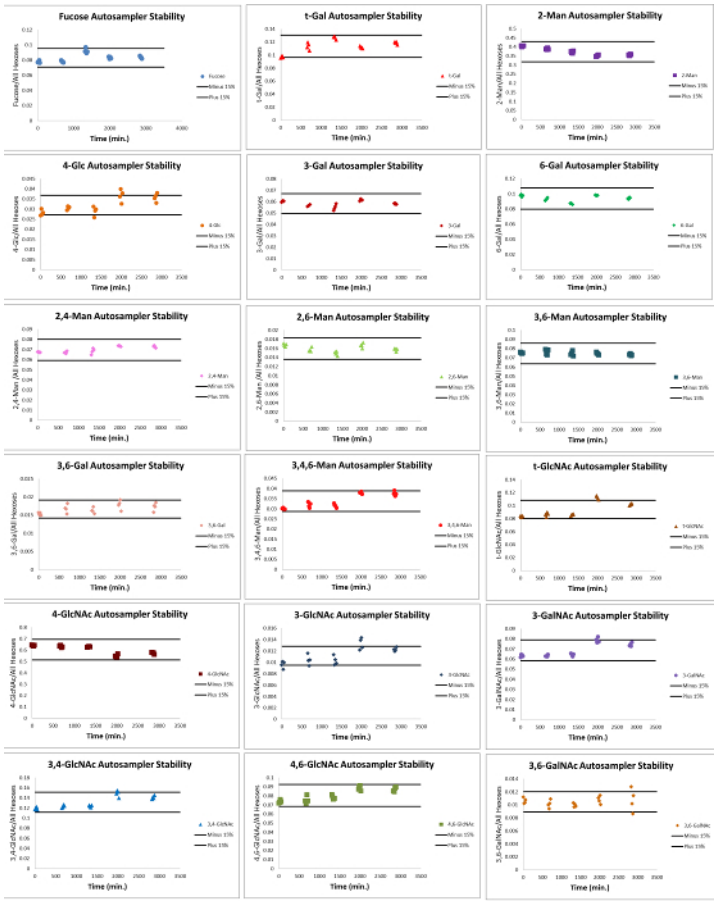

Figure 4. Autosampler Stability. Autosampler stability over 48 hours for the 18 most abundant glycan nodes in human plasma. At 22 hours the sample was completely dried and reconstituted in 120 µl acetone. Each cluster of data points represents four consecutive injections of the same sample. Black lines encompass ± 15% of the average normalized value for each glycan node. Please click here to view a larger version of this figure.

	Normalized to Sum of all Hexoses											Normalized to Sum of all HexNAcs						
	Fucose	t-Gal	2-Man	4-Glc	3-Gal	6-Gal	2,4-Man	2,6-Man	3,6-Man	3,6-Gal	3,4,6-Man	t-GlcNAc	4-GlcNAc	3-GlcNAc	3-GalNAc	3,4-GlcNAc	4,6-GlcNAc	3,6-GalNAc
Average Intra-Assay %CV	6.6	7.8	2.8	13.5	20.2	2.7	6.4	5.8	13.2	20.8	7.4	5.0	2.1	11.7	7.0	7.3	3.3	12.2
Interassay %CV	12.3	7.7	5.3	15.6	26.8	9.8	11.2	6.5	15.7	34.8	19.0	4.9	2.9	20.7	8.7	11.5	6.1	15.4

Table 1. Intra- and interassay reproducibility. Values represent %CV of total hexose or total HexNAc-normalized individual glycan nodes**.** All glycan nodes contributing at least 1% of the total hexose or HexNAc signal are listed. Data were acquired by 3 separate analysts on 3 separate days, using the same stock of EDTA plasma. N = 6 samples per batch. Please click here to download this table as an Excel spreadsheet.

Discussion

In general, the successful production of partially methylated alditol acetates (PMAAs) from hexoses is fraught with fewer difficulties and is more robust than the successful production of *N*-acetylhexosamine (HexNAc) PMAAs. The exact mechanism behind this phenomenon as it plays out in every step of this procedure is unknown, but must relate to the unique chemistry of the *N*-acetyl group (rather than hydroxyl group) that is unique to HexNAcs relative to hexoses. The mechanism behind this phenomenon as it relates to acid hydrolysis is explained elsewhere.[43] In short, the capacity for the *N*-methylacetamido to become positively charged during acid hydrolysis makes the glycosidic linkage resistant to acid hydrolysis. This explains the low yield of HexNAc relative to hexose (11.3% of total HexNAc + hexose signal, rather than 50% of total) as described above for the analysis of *N*-acetyllactosamine. Notably, this relatively lower yield of HexNAcs does not make them difficult to detect in complex biofluids and tissues, or preclude facile detection of glycan nodes derived from large, complex glycans (*e.g.*, 2,4-Man, 2,6-Man, 3,4,6-Man, and 3,4-GlcNAc, **Figure 2**).[33] Given the manner in which XIC peak areas of glycan nodes are normalized (Step 6.3), as long as the relative yield of each individual HexNAc remains consistent relative to other HexNAcs (which it does, see **Table 1**), useful information on the relative quantities of the different HexNAcs between different samples can be obtained. This holds true for hexoses as well. Moreover, we have previously shown that the ratios of hexoses to HexNAcs display consistent quantitative behavior as well[33] — a phenomenon which is continually monitored via incorporation of QC sample(s) in every batch.

The manner in which permethylation is performed has the greatest impact on the overall yield and reproducibility of HexNAc PMAAs. In particular, great care should be taken to completely avoid exposure of permethylated glycans to alkaline aqueous conditions. Two key steps in this regard are 1) leaving all white precipitate in the spin-through solutions behind (Steps 1.3.13 and 1.3.14), and 2) immediately mixing the spin-through solutions once they are added to the phosphate buffer (Steps 1.3.13 and 1.3.14). A buffer rather than simple salt solution is included at this stage and for subsequent liquid/liquid extraction steps to prevent inadvertent alkalinization of the aqueous solution. We suspect that under

Copyright © 2016 Journal of Visualized Experiments

alkaline conditions the acetyl group of the methylated and acetylated 2-amino group of HexNAcs may undergo hydrolysis, resulting in a more polar secondary amine that decreases the overall extraction efficiency of the associated glycan into chloroform.

The most easily recognizable feature of unsuccessfully permethylated HexNAcs is the intensity of the 4-linked GlcNAc (4-GlcNAc) chromatographic peak relative to those of 6-Gal, 3,6-Man, and the baseline intensity of the background during final column bake-out (**Figure 3**). When the absolute abundance of the 4-GlcNAc PMAA is low, its normalized abundance relative to all other HexNAcs also tends to be low, with a concomitant increase (most noticeably) of 3,4-GlcNAc.

A few changes designed to optimize overall yield and assay robustness have been made since our initial publication describing this analytical approach.[33] One of these changes is the way in which the integrated extracted ion chromatograms (XICs) are normalized: For the sake of simplicity, we now divide the area of each individual hexose XIC by the sum of all hexose XIC areas; likewise, the area of each individual HexNAc XIC is divided by the sum of all HexNAc XIC areas. As seen in **Table 1**, overall interassay/inter-analyst reproducibility for all glycan nodes that contribute to > 1% of their respective hexose or HexNAc signal averages 13 %CV.

To our knowledge, this is the only incarnation of truly bottom-up glycomics in which glycans are first broken down and then their components analyzed to construct a quantitative sample-wide portrait of glycan composition. Here, instead of traditional enzymatic release, the permethylation process non-reductively eliminates (releases) *O*-linked glycans from their respective proteins,[40] while *N*-linked glycans are released during acid hydrolysis.[33] As a complementary approach to traditional top-down glycomics, this approach is able to pool unique glycan features of interest such as "core fucosylation", "6-sialylation", "bisecting GlcNAc", and "beta 1-6 branching" into single analytical signals (see, 4,6-GlcNAc, 6-Gal, 3,4,6-Man and 2,6-Man nodes in **Figure 2**, respectively). In traditional top-down approaches, features such as these that ultimately depend on the unique activities of one or two key glycosyltransferases[33] are typically distributed across dozens of intact glycans and can sometimes be difficult or impossible to resolve (*e.g.*, 3-sialylation vs. 6-sialylation) due to the degeneracy of some intact glycan masses. Moreover, the bottom-up approach presented here has demonstrated initial promise in non-invasively detecting lung cancer.[33] Further studies are underway to validate these initial findings, as well as additional, yet unpublished results pertaining to the detection of other forms of cancer.

The greatest limitation of the approach described here is that it is constrained in terms of its limits of detection, if it were to be applied to pre-isolated glycoproteins. Based on unpublished analyses of individual glycan standards without carrier protein, limits of quantification for individual glycans appear to lie in the low microgram range. These are by no means low LOQs in absolute terms, but this fact does not matter with regard to the originally intended scope of the assay-which was not designed for and has no need to achieve low LOQs (at least for the purposes described here and in our previous publication[33]). In fact, human plasma/serum contains glycoproteins in the 10s of mg/ml concentration range-meaning that for the analysis of blood plasma/serum we only inject ~ 1/100th of the final sample volume and split 40 out of 41 parts of that small quantity to waste in the GC injector port. Without this practice, some of the glycan nodes can saturate the detector. Picomole quantities of glycoproteins that can produce adequate intact glycan signals by conventional top-down MALDI-MS or LC-MS based approaches cannot be detected with this approach. Further refinement of the methodology is underway to remedy this limitation.

Disclosures

The authors have nothing to disclose.

Acknowledgements

This work was supported by the College of Liberal Arts and Sciences of Arizona State University in the form of laboratory startup funds to CRB. It was also supported by a grant from Flinn Foundation (Grant No. 1977) and by the National Cancer Institute of the National Institutes of Health under Award Number R33CA191110. JA was supported by the National Institute of General Medical Sciences of the National Institutes of Health Postbaccalaureate Research Education Program (PREP) under award number R25GM071798. The content is solely the responsibility of the authors and does not necessarily represent the official views of the National Institutes of Health.

References

1. Li, M., Song, L., & Qin, X. Glycan changes: cancer metastasis and anti-cancer vaccines. *J Biosciences.* **35** (4), 665-673, (2010).
2. Stanley, P., Schachter, H., & Taniguchi, N. in: *Essentials of Glycobiology.*, *2nd edn.* A. Varki *et al.*, eds., Ch. 8: *N-Glycans.* Cold Spring Harbor Laboratory Press, Cold Spring Harbor, New York (2009).
3. Apweiler, R., Hermjakob, H., & Sharon, N. On the frequency of protein glycosylation, as deduced from analysis of the SWISS-PROT database. *Biochim Biophys Acta.* **1473** (1), 4-8 (1999).
4. Brockhausen, I., Schachter, H., & Stanley, P. in: *Essentials of Glycobiology.*, *2nd edn.* A. Varki *et al.*, eds., Ch. 9: *O-GalNAc Glycans.* Cold Spring Harbor Laboratory Press, Cold Spring Harbor, New York (2009).
5. Rini, J., Esko, J., & Varki, A. in: *Essentials of Glycobiology.*, *2nd edn.* A. Varki *et al.*, eds., Ch. 5: *Glycosyltransferases and Glycan-processing Enzymes.* Cold Spring Harbor Laboratory Press, Cold Spring Harbor, New York (2009).
6. Gercel-Taylor, C., Bazzett, L. B., & Taylor, D. D. Presence of aberrant tumor-reactive immunoglobulins in the circulation of patients with ovarian cancer. *Gynecol Oncol.* **81** (1), 71-76, (2001).
7. An, H. J. *et al.* Profiling of glycans in serum for the discovery of potential biomarkers for ovarian cancer. *J Proteome Res.* **5** (7), 1626-1635, (2006).
8. Kanoh, Y. *et al.* Changes in serum IgG oligosaccharide chains with prostate cancer progression. *Anticancer Res.* **24** (5B), 3135-3139 (2004).
9. Kyselova, Z. *et al.* Alterations in the serum glycome due to metastatic prostate cancer. *J Proteome Res.* **6** (5), 1822-1832, (2007).
10. Okuyama, N. *et al.* Fucosylated haptoglobin is a novel marker for pancreatic cancer: a detailed analysis of the oligosaccharide structure and a possible mechanism for fucosylation. *Int J Cancer.* **118** (11), 2803-2808, (2006).
11. Zhao, J. *et al.* Glycoprotein microarrays with multi-lectin detection: unique lectin binding patterns as a tool for classifying normal, chronic pancreatitis and pancreatic cancer sera. *J Proteome Res.* **6** (5), 1864-1874, (2007).

Copyright © 2016 Journal of Visualized Experiments

12. Comunale, M. A. *et al.* Proteomic analysis of serum associated fucosylated glycoproteins in the development of primary hepatocellular carcinoma. *J Proteome Res.* **5** (2), 308-315, (2006).
13. Goldman, R. *et al.* Detection of Hepatocellular Carcinoma Using Glycomic Analysis. *Clin Cancer Res.* **15** (5), 1808-1813, (2009).
14. Aurer, I. *et al.* Aberrant glycosylation of Igg heavy chain in multiple myeloma. *Coll Antropol.* **31** (1), 247-251 (2007).
15. Abd Hamid, U. M. *et al.* A strategy to reveal potential glycan markers from serum glycoproteins associated with breast cancer progression. *Glycobiology.* **18** (12), 1105-1118, (2008).
16. Kyselova, Z. *et al.* Breast cancer diagnosis and prognosis through quantitative measurements of serum glycan profiles. *Clin Chem.* **54** (7), 1166-1175, (2008).
17. Hongsachart, P. *et al.* Glycoproteomic analysis of WGA-bound glycoprotein biomarkers in sera from patients with lung adenocarcinoma. *Electrophoresis.* **30** (7), 1206-1220, (2009).
18. Arnold, J. N. *et al.* Novel glycan biomarkers for the detection of lung cancer. *J Proteome Res.* **10** (4), 1755-1764, (2011).
19. Bones, J., Mittermayr, S., O'Donoghue, N., Guttman, A., & Rudd, P. M. Ultra performance liquid chromatographic profiling of serum N-glycans for fast and efficient identification of cancer associated alterations in glycosylation. *Anal Chem.* **82** (24), 10208-10215, (2010).
20. Kodar, K., Stadlmann, J., Klaamas, K., Sergeyev, B., & Kurtenkov, O. Immunoglobulin G Fc N-glycan profiling in patients with gastric cancer by LC-ESI-MS: relation to tumor progression and survival. *Glycoconj J.* **29** (1), 57-66, (2012).
21. Chen, G. *et al.* Human IgG Fc-glycosylation profiling reveals associations with age, sex, female sex hormones and thyroid cancer. *J Proteomics.* **75** (10), 2824-2834, (2012).
22. Takeda, Y. *et al.* Fucosylated haptoglobin is a novel type of cancer biomarker linked to the prognosis after an operation in colorectal cancer. *Cancer.* **118** (12), 3036-3043, (2012).
23. Parekh, R. B. *et al.* Association of rheumatoid arthritis and primary osteoarthritis with changes in the glycosylation pattern of total serum IgG. *Nature.* **316** (6027), 452-457, (1985).
24. Mehta, A. S. *et al.* Increased levels of galactose-deficient anti-Gal immunoglobulin G in the sera of hepatitis C virus-infected individuals with fibrosis and cirrhosis. *J Virol.* **82** (3), 1259-1270, (2008).
25. Horvat, T., Zoldoš, V., & Lauc, G. Evolutional and clinical implications of the epigenetic regulation of protein glycosylation. *Clinical Epigenetics.* **2** (2), 425-432, (2011).
26. Zoldoš, V., Novokmet, M., Bečeheli, I., & Lauc, G. Genomics and epigenomics of the human glycome. *Glycoconj J.* **30** (1), 41-50, (2013).
27. Lowe, J. B., & Marth, J. D. A genetic approach to Mammalian glycan function. *Annu Rev Biochem.* **72**, 643-691, (2003).
28. Tuccillo, F. M. *et al.* Aberrant Glycosylation as Biomarker for Cancer: Focus on CD43. *Biomed Res Int.*, (2014).
29. Varki, A., Kannagi, R., & Toole, B. in: *Essentials of Glycobiology.*, *2nd edn.* A. Varki *et al.*, eds., Ch. 44: *Glycosylation Changes in Cancer.* Cold Spring Harbor Laboratory Press, Cold Spring Harbor, New York (2009).
30. Brockhausen, I. Mucin-type O-glycans in human colon and breast cancer: glycodynamics and functions. *EMBO reports.* **7** (6), 599-604, (2006).
31. Ohtsubo, K., & Marth, J. D. Glycosylation in cellular mechanisms of health and disease. *Cell.* **126** (5), 855-867, (2006).
32. Bertozzi, C. R., & Sasisekharan, R. in: *Essentials of Glycobiology.*, *2nd edn.* A. Varki *et al.*, eds., Ch. 48: *Glycomics.* Cold Spring Harbor Laboratory Press, Cold Spring Harbor, New York (2009).
33. Borges, C. R., Rehder, D. S., & Boffetta, P. Multiplexed surrogate analysis of glycotransferase activity in whole biospecimens. *Anal Chem.* **85** (5), 2927-2936, (2013).
34. Mcinnes, A. G., Ball, D. H., Cooper, F. P., & Bishop, C. T. Separation of Carbohydrate Derivatives by Gas-Liquid Partition Chromatography. *J Chromatogr.* **1** (6), 556-557, (1958).
35. Ciucanu, I., & Caprita, R. Per-O-methylation of neutral carbohydrates directly from aqueous samples for gas chromatography and mass spectrometry analysis. *Anal Chim Acta.* **585** (1), 81-85, (2007).
36. Ciucanu, I., & Kerek, F. A simple and rapid method for the permethylation of carbohydrates. *Carbohydr Res.* **131**, 209-217, (1984).
37. Kang, P., Mechref, Y., Klouckova, I., & Novotny, M. V. Solid-phase permethylation of glycans for mass spectrometric analysis. *Rapid Commun Mass Sp.* **19** (23), 3421-3428, (2005).
38. Kang, P., Mechref, Y., & Novotny, M. V. High-throughput solid-phase permethylation of glycans prior to mass spectrometry. *Rapid Commun Mass Sp.* **22** (5), 721-734, (2008).
39. Goetz, J. A., Mechref, Y., Kang, P., Jeng, M. H., & Novotny, M. V. Glycomic profiling of invasive and non-invasive breast cancer cells. *Glycoconj J.* **26** (2), 117-131, (2009).
40. Goetz, J. A., Novotny, M. V., & Mechref, Y. Enzymatic/chemical release of O-glycans allowing MS analysis at high sensitivity. *Anal Chem.* **81** (23), 9546-9552, (2009).
41. Mulloy, B., Hart, G. W., & Stanley, P. in: *Essentials of Glycobiology.*, *2nd edn.* A. Varki *et al.*, eds., Ch. 47: *Structural Analysis of Glycans.* Cold Spring Harbor Laboratory Press, Cold Spring Harbor, New York (2009).
42. Seed, B. Silanizing glassware. *Curr Protoc Immunol.* **21**, A.3K.1-A.3K.2, (1997).
43. Stellner, K., Saito, H., & Hakomori, S. I. Determination of aminosugar linkages in glycolipids by methylation. Aminosugar linkages of ceramide pentasaccharides of rabbit erythrocytes and of Forssman antigen. *Arch Biochem Biophys.* **155** (2), 464-472 (1973).

Copyright © 2016 Journal of Visualized Experiments